that are generally used to evaluate the technological strength (weldability).

2. Any deterioration of properties occurring with time under certain conditions of thermal-load and additional effects on metal, which are characteristic of welding, leads to a limiting state of metal, which causes formation of discontinuities of an inter- or transcrystalline character and degradation.

3. The degradation of properties of metal of the joint should be regarded as a universal criterion for evaluation of the technological strength and, hence, weldability.

1. Yushchenko, K.A., Derlomenko, V.V. (2005) Analysis of modern views on weldability. *The Paton Welding J.*, **1**, 5–9.
2. Yushchenko, K.A., Derlomenko, V.V. (2005) Materials weldability criteria. *Ibid.*, **8**, 68–70.
3. Yushchenko, K.A., Derlomenko, V.V. (2006) Weldability and changes in physical-mechanical properties of welded joints. *Fiziko-Khimich. Mekhanika Materialiv*, **2**, 89–93.
4. (1979) *Welding in machine-building*: Refer. Book. Vol. 3. Moscow: Mashinostroenie.
5. Shorshorov, M.Kh., Erokhin, A.A., Chernyshova, T.A. et al. (1973) *Hot cracks in welding of heat-resistant alloys*. Moscow: Mashinostroenie.
6. (1991) *Welding and materials to be welded*. Vol. 1: Weldability of materials: Refer. Book. Ed. by E.L. Makarov. Moscow: Metallurgiya.
7. Stout, R.D., Dorville, W.D. (1978) *Weldability of steels*. New York: Welding Res. Council.
8. Hrivnak, I. (1984) *Weldability of steels*. Ed. by E.L. Makarov. Moscow: Mashinostroenie.
9. Wilken, K. (1998) Investigation to compare hot cracking tests of externally loaded specimen. *IIW Doc. IX-1923–98*.
10. Savage, W.F., Zuntic, C.D. (1965) The Varestraint Test. *Welding J.*, 44(**10**), 433–442.
11. Nissley, N.E., Lippold, J.C. (2003) Development of the strain-to-fracture test for evaluating ductility-dip cracking in austenitic alloys. *Ibid.*, 82(**12**), 355–364.
12. Shorshorov, M.Kh., Chernyshova, T.A., Krasovsky, A.I. (1972) *Weldability tests of metals*. Moscow: Metallurgiya.
13. Kamoi, K., Machora, Y., Ohmosy, Y. (1986) Effect of stacking fault precipitation on hot deformation of austenitic stainless steel. *Transact. of ISIY*, 26(**2**), 159–166.
14. Yushchenko, K.A., Savchenko, V.S., Chervyakov, N.O. et al. (2010) Probable mechanism of cracking of stable-austenitic welds caused by oxygen segregation. *The Paton Welding J.*, **5**, 5–9.
15. Savchenko, V.S., Yushchenko, K.A., Zvjagintseva, A.V. et al. (2007) Investigation of structure and crack formation in welded joints of single crystal Ni-base alloys. *Welding in the World*, 51(**11/12**), 76–81.

TREATMENT OF THE SURFACE OF ALUMINIUM-MATRIX COMPOSITE MATERIALS BY CONCENTRATED ENERGY SOURCES

N.V. KOBERNIK[1], **G.G. CHERNYSHOV**[1], **R.S. MIKHEEV**[2] and **T.A. CHERNYSHOVA**[2]
[1]N.E. Bauman Moscow State Technical University, Moscow, RF
[2]A.A. Baikov Institute of Metallurgy, RAS, Moscow, RF

Studied was the possibility of modifying surface layers of antifriction aluminium alloy AK9 and aluminium-matrix composite materials reinforced with particles of silicon carbide SiC and aluminium oxide Al_2O_3 in melting of surfaces with arc discharge in magnetic field, as well as with pulsed laser beam. It is shown that surface melting is accompanied by substantial dispersion of the initial surface layer structure. Samples after treatment are characterized by mechanical and tribological properties that are superior to those of the initial material.

Keywords: *arc surface melting, pulsed laser radiation, reinforced composite materials, magnetic field, modified surfaces*

At present designers are showing interest in aluminium-matrix composite materials (CM) reinforced by refractory ceramic particles. Above-mentioned CM are characterized by high wear resistance and tribological properties, making them promising for application in tribounits [1, 2]. A highly important direction of further work is producing wear-resistant antifriction coatings from these CM on parts operating under extreme conditions. Studies [3–8] show the possibility of producing wear-resistant coatings from such materials by argon-arc surfacing with application of filler rods, the deposited coatings being characterized by service properties close to those of cast CM of the same composition. There is a further possibility of improvement of service properties of surface layer of initial CM and deposited coatings by modifying their

structure, as a change of dimensions of structural elements markedly influences the part wear resistance [9].

In [10, 11] it is proposed to apply microplasma discharges, as well as electron beam and laser radiation for modifying the surface. However, such methods of CM surface treatment are not always cost-effective, because of the low treatment speed, as well as the need for application of complex and expensive equipment. In addition, microplasma treatment in vacuum chambers is related to limitations in product dimensions, and in laser treatment it is also necessary to take into account the reflecting properties of the treated material. A more cost-effective and flexible process of CM surface treatment is arc surface melting with magnetic field impact on the arc and molten pool, allowing high-quality dense surface layers of homogeneous composition to be produced [12].

This work presents the results of investigation of the possibilities of arc surface melting in a magnetic

field, as well as surface melting by pulsed laser radiation for modifying the surface layers of cast samples from aluminium alloy AK9 and aluminium-matrix CM strengthened by particles of silicon carbide SiC and aluminium oxide Al_2O_3.

At modifying of surface layers of aluminium-matrix CM, reinforced by particles of silicon carbide by surface melting, reinforcing phase degradation due to CM melt overheating is possible [13]. This is manifested in formation of a considerable amount of interphase reaction products Al_4C_3 and Al_4SiC_4, this leading to shape loss as a result of corrosion failure in the presence of water vapours, and lowering of CM strength and rigidity. In [3, 14] it is shown that the processes of reinforcing phase degradation can be suppressed at rational selection of treatment modes, surfacing technique and using alloys of Al–Si system with 11–13 wt.% Si as matrix. Therefore, investigations were performed using CM with AK12M2MgN and AK12 matrix alloys and modes recommended in [3–6, 14].

Experiments on modification of surface layer structure by surface melting were conducted on cast plates of aluminium alloy AK9 (GOST 1583–93) of the following composition, wt.%: 9–11 Si; ≤ 1 Cu; 0.2–0.4 Mg; 0.2–0.5 Mn; ≤ 0.3 Ni; ≤ 0.5 Zn; ≤ 1.3 Fe; Al being the base, and dispersion-strengthened aluminium-matrix CM.

Dispersion-strengthened CM were produced by mechanical mixing of reinforcing filler into the matrix melt. CM matrix were aluminium alloys (GOST 1583–93) AK12M2MgN of the following composition, wt.%: 11–3 Si; 1.5–3.0 Cu; 0.3–0.6 Mn; 0.85–1.35 Mg; < 0.5 Zn; 0.05–1.2 Ti; 0.3–1.3 Ni; < 0.8 Fe; < 0.2 Cr; < 0.1 Sn; and AK12: 10–13 Si; < 0.6 Cu; < 0.5 Mn; < 0.1 Mg; < 0.3 Zn; < 0.7 Fe; < 0.1 Ni; < 0.1 Ti; Al being the balance. Fillers were particles of silicon carbide SiC and aluminium oxide Al_2O_3. Mean diameter of SiC particles was equal to 14 and 28 μm, and for Al_2O_3 it was 40 μm. Before mixing the powders were soaked in an oven for drying, burning out accidental organic contamination and oxidation of free silicon. Powder mixing into the melt was performed by pan-type mixer. CM plates were produced by pouring the composite melt into the mould.

Surface melting by arc discharge in magnetic field of surface layer of cast samples was performed by an arc running in argon between tungsten electrode and item at straight polarity direct current in the center of a four-pole magnetic system [12]. Arc current was I_a = 100 A, surface melting rate — $v_{s.m}$ = 14 m/h, magnetic induction b = 0.048–0.120 T.

Surface melting by pulsed laser radiation was performed in QUANT-15 unit with pulse power W_p = = 815, 1500 and 2250 W and degree of defocusing (or distance from beam focus to sample surface) Δf = 1, 3 and 5 mm, providing heated spot diameter d_s = 0.3, 0.9 and 1.5 mm at lens focal distance of 0.5 mm. Pulse time t_p was set at 4 ms, and pulse frequency F_p = = 1 Hz. Surface melting rate was selected so as to ensure point overlap factor K_{ov} = S/d_s = 0.5, where S is the step at superposition of individual spots, argon being used as shielding gas.

Modified surface structure was studied in Leica DMILM optical microscope using image analysis program Qwin, as well as in scanning electron microscopes Leo 430i and FEI Quanta 3D FEG fitted with attachments for X-ray microprobe analysis (XRMPA).

Mechanical properties were determined by measurement of microhardness by depth of deposited metal in Wilson Wolpert 432SVD instrument at the load of 0.5 N, as well as measurement of Brinell hardness in an all-purpose Wilson Wolpert 930 N instrument by indendation of 2.5 mm sphere at 620 N load.

To assess modification effectiveness dry sliding friction tests of as-cast initial samples and those after surface melting by an arc in magnetic field were conducted. Friction was performed in MTU-01 unit (TU 4271-001-29034600–2004) by the following schematic: rotating bushing (counterbody from steel 40Kh with more than HRC 45 hardness) over washer (samples from CM with modified surface) at 18–60 N load and sliding velocity of 0.39 m/s. Testing included registering the moment of friction and mass change
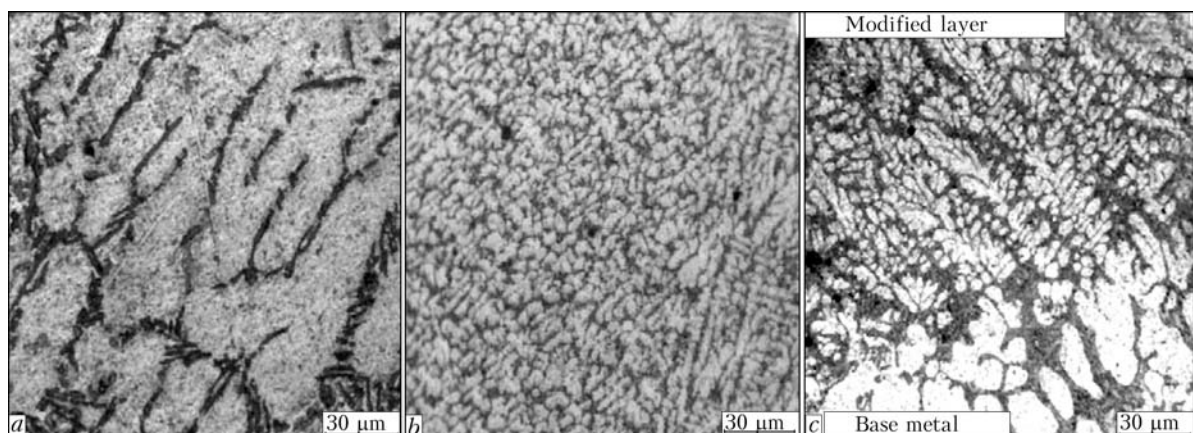

Figure 1. Microstructures of AK9 alloy in the initial (cast) condition (*a*), of upper part of modified layer (*b*) and fusion line (*c*) after treatment by an arc in the magnetic field (*b* = 0.048 T)

by weighing each sample before and after testing with the accuracy of $\pm(0.5 \cdot 10^{-3})$ g. First stage of triboloading of 15 min duration at the load of 18 N and sliding velocity of 0.39 m/s was regarded to be running-in one.

Sample behaviour during dry sliding friction was assessed by bulk intensity of wear I_V, friction coefficient f_{fr}, wear coefficient K and stability coefficient α_{st}. Values of these parameters were determined by the following formulas [15, 16]:

$$I_V = \frac{\Delta m}{\rho L}; \qquad (1)$$

$$f_{fr} = \frac{M}{R_m F_1}; \qquad (2)$$

$$K = \frac{I_V H}{F_1}; \qquad (3)$$

$$\alpha_{st} = \frac{f_m}{f_{max}}, \qquad (4)$$

where ρ is the sample metal density, g/mm^3; L is the friction path, m; M is the moment of friction, N·m; R_m is the mean radius of the counterbody, mm; F_1 is the applied load, N; H is the sample metal hardness, MPa; f_m, f_{max} are the mean and maximum friction coefficients.

Stability coefficient α_{st} is a dimensionless value and characterizes stability of the process of dry sliding friction. Wear coefficient K, which is also a dimensionless value, expresses the probability of worn particle separation at friction.

Structure and mechanical properties of surface layers melted by arc discharge in the magnetic field. Microstructures of samples from AK9 alloy and dispersion-filled CM AK12 + 10 % Al$_2$O$_{3(40)}$ and AK12M2MgN + 12 % SiC$_{(14)}$ in the initial condition are shown in Figure 1, *a* and Figure 2, *a, d*, respectively. It is seen from the Figures that the cast structure of AK9 alloy consists of coarse cellular-dendritic crystals of α-Al of thickness λ = 30−50 μm and interdendritic eutectic interlayers. According to XRMPA these interlayers, in addition to α-Al and eutectic silicon also contain nickel, iron and copper aluminides. Thickness λ of α-Al crystals of CM initial (cast) structure is equal to 13−15 μm (AK12 + 10 % Al$_2$O$_{3(40)}$) and 20−25 μm (AK12M2MgN + 12 % SiC$_{(14)}$), which is somewhat smaller than in AK9 aluminium alloy. This is the consequence of the influence of reinforcing Al$_2$O$_3$ and SiC particles, limiting the volumes of melts, in which liquation occurs.

Samples obtained after arc surface melting in a magnetic field are characterized by a sufficiently smooth surface. Influence of magnetic induction on the shape of surface layers, obtained by arc melting under the impact of magnetic field on the arc, was
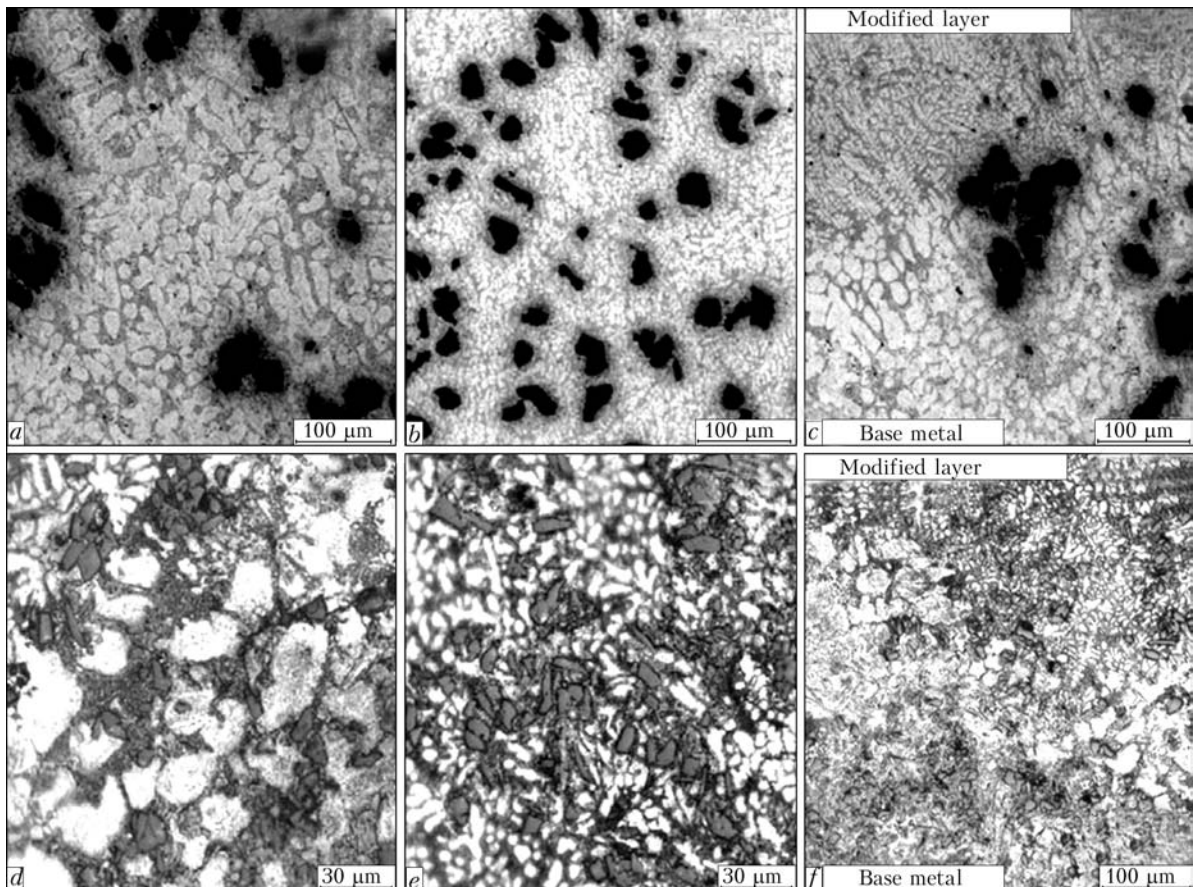

Figure 2. Microstructures of CM AK12 + 10 % Al$_2$O$_{3(40)}$ (*a−c*) and AK12M2MgN + 12 % SiC$_{(14)}$ (*d−f*) in the initial (cast) condition (*a, d*), of upper part of modified layer (*b, e*) and fusion line (*c, f*) after treatment by an arc in a magnetic field (I_w = 110 A; U_a = 16 V; b = 0.048 T)

Table 1. Geometrical dimensions of welds made on samples from different materials and at different values of magnetic induction

Sample material	B, mm	h, mm	B, mm	h, mm
	b = 0.048 T		b = 0.120 T	
AK9	7.00	1.20	8.50	0.50
AK12 + 10 % $Al_2O_{3(40)}$	6.73	1.27	9.27	1.67
AK12M2MgN + 12 % $SiC_{(14)}$	6.60	2.00	8.07	2.40

studied on transverse macrosections of surface-melted samples. Measurements of geometrical dimensions of welds showed that all the materials are characterized by increase of width B and surface melting zone at increase of magnetic induction (Table 1), as a higher degree of arc defocusing is achieved. Change of penetration depth h depending on magnetic induction is not so evident, but the tendency to its decrease is preserved.

Microstructures of samples from AK9 alloy after modifying treatment by an arc discharge in the magnetic field are shown in Figure 1, *b, c*. The Figures show a considerable dispersion of the initial structure caused by high rates of cooling of the thin layer of molten metal. Parameter λ decreases to 5—7 μm (Figure 1, *b*). Near the fusion line the dispersity of the surface melted layer structure is somewhat lower as a result of partial inheritance of substrate structure at epitaxial solidification, as well as lower initial rate of melt solidification (Figure 1, *c*).

Figure 2, *b, c, e, f* shows microstructures of samples from dispersion-filled CM of AK12 + 10 % $Al_2O_{3(40)}$ and AK12M2gN + 12 % $SiC_{(14)}$ compositions, respectively. Surface treatment of samples by arc melting with the impact of magnetic field on the arc results in refinement of the initial matrix structure (thickness is equal to 3—4 and 4—5 μm, respectively). Volume fraction and size of reinforcing Al_2O_3 and SiC particles do not change.

SiC particles in treated surface layers of a sample of AK12M2MgN + 12 % $SiC_{(14)}$ CM preserve their initial cleavage faceting, which is indicative of an absence of intensive interphase interaction between filler and matrix melt during arc surface melting (Figure 2, *b, e*). In addition, redistribution of reinforcing particles occurs during surface treatment. The high cooling rate, inherent to this technological process, leads to a uniform distribution of reinforcing particles in the matrix (Figure 3).

Table 2. Composition across the depth of treated layer of AK12M2MgN + 12 % $SiC_{(14)}$ CM (XRMPA)

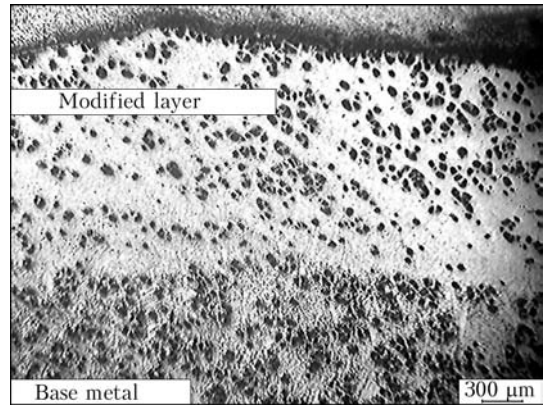| Measured section	Al, wt.% (at.%)	Si, wt.% (at.%)
Base metal	91.58 (91.88)	8.42 (8.12)
Near the fusion line (from modified layer side)	96.30 (96.44)	3.70 (3.56)
Near the surface	83.08 (83.63)	16.92 (16.37)

Figure 3. Macrostructure of AK12 + 10 % $Al_2O_{3(40)}$ CM after treatment by an arc in a magnetic field (I_w = 110 A; U_a = 16 V; b = = 0.120 T)

As a result of treatment the composition across the surface layer thickness changes. Near the fusion line silicon content in the layer decreases, and the zone adjacent to the sample surface is noticeably enriched in silicon compared to the initial structure (Table 2). This is caused by liquation characteristic for directional solidification of the surface-melted layer from the fusion line towards the layer surface.

Refinement of matrix structure and increase of uniformity of filler distribution in the surface layers of dispersion-filled CM after modifying treatment leads to increased hardness of surface layers compared to the initial state of AK9 alloy and dispersion-filled CM (Figure 4). Change of magnetic induction values from 0.048 up to 0.120 T practically does not affect the hardness of surface-melted layer.

Modification of the structure of aluminium alloys and CM by surface treatment by arc melting in a magnetic field improves their wear resistance and tribological characteristics. Values of bulk intensity of wear I_v and wear coefficient K, both for AK9 model sample and for dispersion-filled CM decrease significantly, particularly at increase of the load (Figure 5). This may be due to refinement of dimensions of silicon crystals and relative dimensions of sections of aluminium-based solid solution, increasing the resistance to abrasive and adhesion wear of samples [9]. Absence of degradation of reinforc-
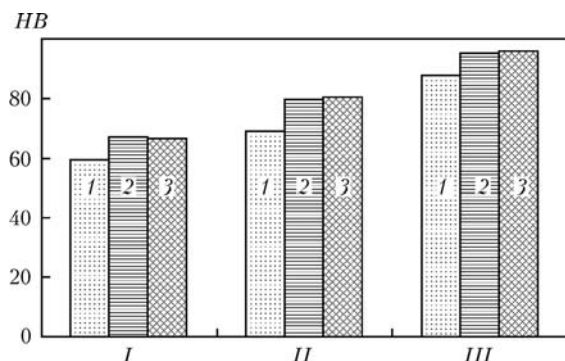

Figure 4. Hardness of samples from AK9 alloy and dispersion-strengthened CM AK9 (*I*), AK12 + 10 % $Al_2O_{3(40)}$ (*II*) and AK12M2MgN + 12 % $SiC_{(14)}$ (*III*) in the initial condition (*1*) and after treatment by the arc in a magnetic field at b = 0.048 (*2*) and 0.120 (*3*) T
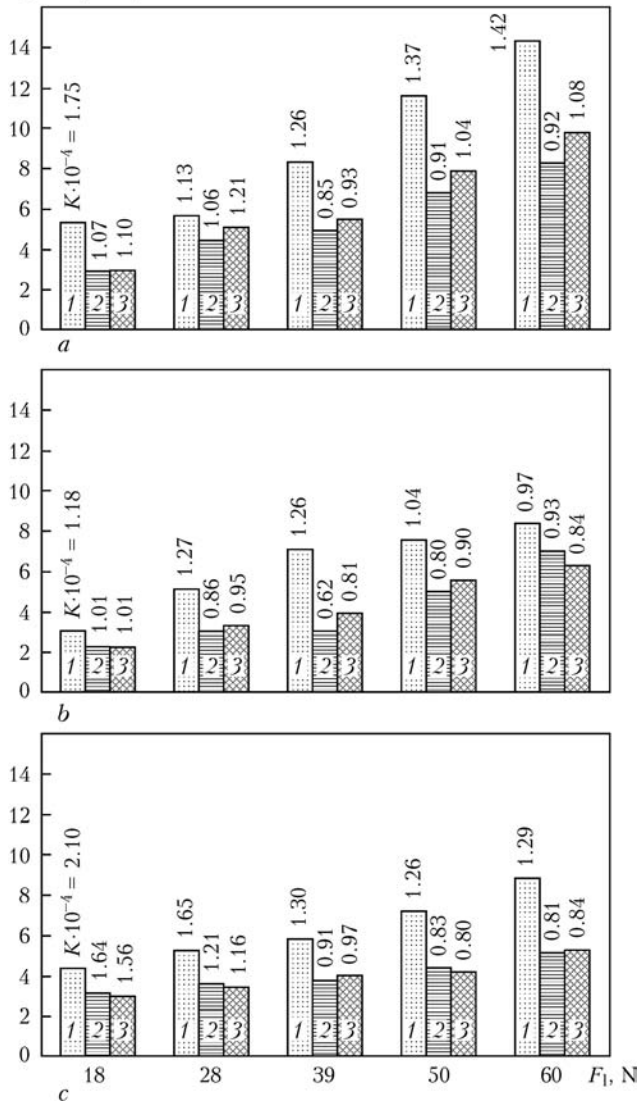
$I_v \cdot 10^{-3}$, mm³/m

Figure 5. Change of bulk wearing intensity I_v and wear coefficient $K \cdot 10^{-4}$ of samples from AK9 alloy (*a*), CM AK12 + 10 % $Al_2O_{3(40)}$ (*b*) and AK12M2MgN + 12 % $SiC_{(14)}$ (*c*) depending on load F_1 under the conditions of dry sliding friction: *1* — initial state; *2, 3* — after modification of the surface layer at $b = 0.048$ and 0.120 T

f_{mod}/f_{in}

Figure 6. Change of normalised friction coefficient f_{mod}/f_{in} of samples of AK9 (*a*), CM AK12 + 10 % $Al_2O_{3(40)}$ (*b*) and AK12M2MgN + + 12 % $SiC_{(14)}$ (*c*) after modifying treatment depending on applied axial load at $b = 0.048$ (*1*) and 0.120 (*2*) T

ing particles in the deposited layers of dispersion-filled CM also has an important role.

Normalized friction coefficients of samples (f_{mod}/f_{in} is the ratio of friction coefficient of modified sample to friction coefficient of initial sample) depending on the applied load are given in Figure 6. It is seen from the Figure that in the entire range of triboloading modified samples from AK9 model alloy have equal or smaller values of friction coefficient compared to cast samples (Figure 6, *a*). Modified dispersion-filled CM feature a somewhat higher friction coefficient at the initial stages of testing at up to 39 N load compared to the initial condition. However, at high loads the values of friction coefficients become similar (Figure 6, *b, c*) that may be related to formation of a transition layer close in composition and dispersity during dry sliding friction process.

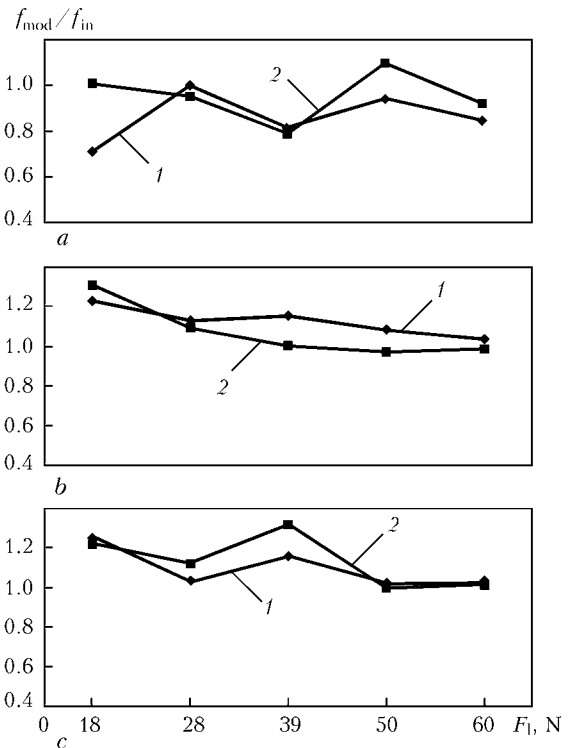During dry sliding friction the subsurface layers are exposed to strong plastic deformation, traces of

which in the form of rotation of dendrite axes in the sliding direction can be observed on transverse microsections of the samples after friction tests (Figure 7, *a*). Width of plastic deformation zone of CM cast samples is equal to about 250 μm, and that of modified samples decreases to 150 μm. At testing at axial load of 60 N a transition layer formed during friction is clearly visible on contact surfaces of the modified sample. According to XRMPA it is a mechanical nanostructured mixture of the material of counterbody and tested sample, as well as their oxides (Figure 7, *b*). Appearance of iron or its oxides can be due to abrasive impact on the counterbody of reinforcing dispersed particles of Al_2O_3, SiC, as well as silicon crystals in the composition of AK9 and AK12M2MgN alloys. The more finely-dispersed is the microstructure of the sample tested by friction, the more intensive are the processes of nanostructuring in the transition layer, which promotes lowering of friction coefficient and protects the sample from wear.

Initial samples, as well as samples after modifying treatment, are characterized by the coefficient of stability of the process of sliding friction without lubrication close to a unity (Table 3), which is inherent to antifriction materials and is indicative of friction process stability. It is seen that surface melting by an arc in the magnetic field leads to an increase of the coefficient of stability of samples from dispersion-filled CM, its high values (not lower than 0.9) being preserved even at maximum axial loads.

Structure and mechanical properties of surface layers melted by pulsed laser radiation. Surfaces
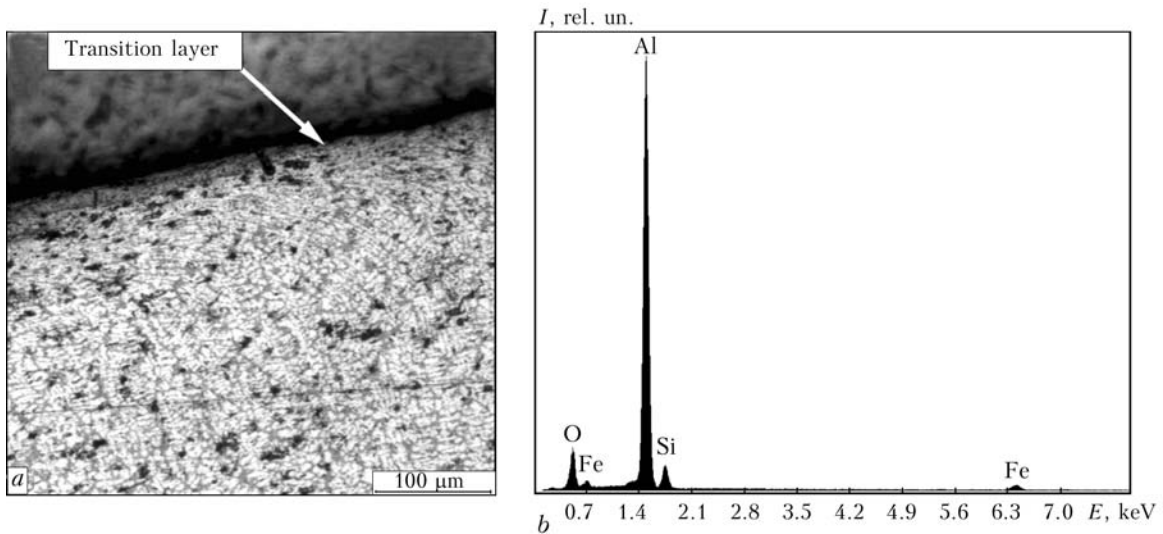
Figure 7. Microstructure of modified sample from AK9 alloy after friction tests (*a*) and elemental composition of the transition layer according to XRMPA (*b*)

melted at the smallest value of beam defocusing ($\Delta f =$ = 1 mm or d_s = 0.3 mm) have pronounced roughness and a multitude of dents in the entire range of studied values of pulse energy. Such a state of melted surface is indicative of exceeding the optimum density of laser radiation E_{opt}. Such exceeding results in formation of a considerable fraction of vapour-gas phase, leading to considerable spattering and evaporation of base metal. Melted surfaces, obtained at defocusing $\Delta f =$ = 3 and 5 mm, have a smooth surface. Width of the strip molten in one pass is not more than 1.5 mm.

Figure 8 shows microstructures of samples from AK12M2MgN + 5 % SiC$_{(28)}$ CM surface-melted by pulsed laser radiation. In CM melted surface layer the reinforcing phase is present and the particles preserve their dimensions and cleavage faceting in the entire range of the studied modes. λ values in different modes of laser surface melting for $\Delta f = 1/3$ mm are given below:

W_p, W	812.5	1500	2250
λ, µm	1.90/1.90	1.80/1.70	1.54/1.60

Treatment by laser beam results in refining of the initial structure of the matrix by an order and more (in as-cast condition CM has λ = 30 µm).

In addition to metallographic investigations of the metal of beads produced by surface melting, their hardness measurement was also performed at the degree of defocusing $\Delta f = 1$ mm, and also in the base metal at 5 mm distance from the fusion line (it is equal to HV 130 MPa). Results of hardness measurement are given below:

W, W	815	1500	2250
HV, MPa	161	175	180

Obtained results show that microhardness increases with increase of pulse power, which is the consequence not only of refinement of matrix alloy structure after laser surface melting, but also additional alloying of the matrix by the reinforcing phase.

Degree of refinement of the structure of aluminium-matrix CM at surface melting by pulsed laser radiation is higher than in surface melting by an arc

Table 3. Values of stability coefficients α_{st} of dry sliding friction of samples in the initial condition and after treatment by welding arc in a magnetic field

| Sample material	Treatment state and mode	α_{st} at applied axial load F_l, N				
		18	28	39	50	60
AK9	Initial	0.87	0.91	0.92	0.93	0.90
	Treatment at b = 0.048 T	0.93	0.84	0.85	0.82	0.85
	Treatment at b = 0.120 T	0.87	0.81	0.82	0.85	0.84
AK12 + 10 % Al$_2$O$_{3(40)}$	Initial	0.94	0.93	0.86	0.88	0.81
	Treatment at b = 0.048 T	0.81	0.85	0.95	0.95	0.97
	Treatment at b = 0.120 T	0.95	0.87	0.98	0.94	0.98
AK12M2MgN + 12 % SiC$_{(14)}$	Initial	0.98	0.91	0.91	0.88	0.85
	Treatment at b = 0.048 T	0.98	0.91	0.95	0.94	0.89
	Treatment at b = 0.120 T	0.96	0.94	0.93	0.95	0.93
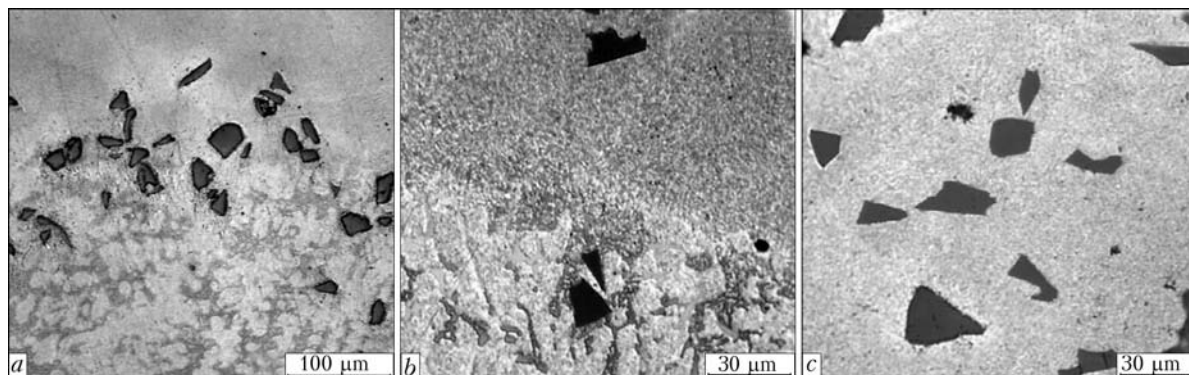
Figure 8. Microstructures of AK12M2MgN + 5 % SiC$_{(28)}$ CM after treatment by pulsed laser radiation (Δf = 1 mm; W_p = 2250 W): *a, b* — fusion line; *c* — central part

discharge in a magnetic field. However, the efficiency of arc surface melting is much higher (minimum width of surface melted strip at arc melting is equal to 6.6 mm with the above treatment method at the speed of 14 m/h, and at laser treatment at the speed of 2.7 m/h it is 1.5 mm).

CONCLUSIONS

1. Possibility of modification of surface layers of aluminium alloy AK9 and aluminium-matrix CM at arc melting of the surface in magnetic field and surface melting by pulsed laser radiation is shown.

2. At treatment of AK9 alloy by arc surface melting in a magnetic field, parameter λ decreases more than 7 times, for AK12 + 10 % Al$_2$O$_{3(40)}$ CM — 4 times, at treatment of AK12M2MgN + 12 % SiC$_{(14)}$ CM — more than 5 times. Application of four-pole magnetic system allows adjustment of geometrical dimensions of surface melting zone (width and depth) and dispersity of the produced structure.

3. At surface melting by pulsed radiation a greater refinement of CM structure is observed. λ parameter for AK12M2MgN + 5 % SiC$_{(28)}$ after laser treatment decreases 16 times, however, surface melting process efficiency is much lower than at arc treatment.

4. Treated surfaces acquire mechanical and tribotechnical characteristics superior to those of the initial material.

5. Process of arc surface melting with impact of a magnetic field on the arc and the melt can be applied to produce high-quality wear-resistant surface layers from aluminium-matrix CM of a uniform composition.

1. Chernyshova, T.A., Kobeleva, L.I., Bolotova, L.K. (2001) Discretely reinforced composites with aluminium alloy matrices and their tribological properties. *Metally*, **6**, 85−98.
2. Chernyshova, T.A., Kobeleva, L.I., Bolotova, L.K. et al. (2005) Behavior in dry sliding friction of dispersion filled composites on the base of aluminium alloys with different level of strength. *Perspect. Materialy*, **5**, 38−44.
3. Kobernik, N.V., Brodyagina, I.V., Chernyshov, G.G. et al. (2005) Argon arc cladding of dispersion-strengthened aluminium matrix composites. *Fizika i Khimiya Obrab. Materialov*, **4**, 67−71.
4. Kobernik, N.V. (2008) Production of wear-resistant coatings by argon arc cladding of matrix of aluminium alloy AK12M2MgN particles SiC. *Zagot. Pr-va v Mashinostroenii*, **3**, 13−17.
5. Kobernik, N.V. (2008) Argon arc cladding of composites of Al−SiC system. *Izvestiya Vuzov. Mashinostroenie*, **2**, 74−80.
6. Kobernik, N.V., Chernyshov, G.G., Mikheev, R.S. et al. (2009) Argon arc cladding of wear-resistant composite coatings. *Fizika i Khimiya Obrab. Materialov*, **1**, 51−55.
7. Kobernik, N.V. (2009) Producing of wear-resistant coatings of Al−SiC system composites by argon arc cladding. *Svarka i Diagnostika*, **1**, 25.
8. Kobernik, N.V., Chernyshov, G.G., Mikheev, R.S. et al. (2009) Influence of method of filler material producing on formation of composite deposited coatings. *Ibid.*, **4**, 18−22.
9. Stroganov, S.B., Rotenberg, V.A., Gershman, G.B. (1977) *Alloys of aluminium with silicon*. Moscow: Metallurgiya.
10. Lapteva, V.G., Kuksenova, L.I., Ivanov, V.A. et al. (2008) Effect of microplasma treatment on properties of near-surface layer of specimens of different structural materials. In: *Proc. of Sci.-Techn. Conf. on Tribology for Machine Building* (Moscow, 2008). CD-ROM, Sect. 3, **19**.
11. Biryukov, V.P. (2008) Laser hardening of friction surfaces by high-power gas, solid-state and fiber lasers. *Ibid.*, **7**.
12. Akulov, A.I., Bul, B.K., Chernyshov, G.G. et al. *Magnetic system*. USSR author's cert. 654964. Publ. 1979.
13. Chernyshova, T.A., Kobeleva, L.I., Shebo, P. et al. (1993) *Interaction of metal melts with reinforcing filler materials*. Moscow: Nauka.
14. Mikheev, R.S., Kobernik, N.V., Chernyshov, G.G. et al. (2006) Effect of pulse laser radiation on structure and properties of aluminium-matrix composites. *Fizika i Khimiya Obrab. Materialov*, **6**, 17−22.
15. Chichinadze, A.V., Berliner, E.M., Braun, E.D. et al. (2003) *Friction, wear and lubrication (tribology and triboengineering)*. Moscow: Mashinostroenie.
16. Fuks, I.G., Buyanovsky, I.A. (1995) *Introduction to tribology*: Manual. Moscow: Neft i Gaz.